Climate changes and Neolithic human migration out-of-Taiwan

Lionel L. SIAME[1a,b,c] and Guillaume LEDUC[a]

[a] **Aix Marseille Univ, CNRS, IRD, INRA, Coll France, CEREGE, Aix-en-Provence, France**

[b] Institute of Earth Sciences, Academia Sinica, P.O. Box 1-55, 128, Sec. 2, Academia Road, Nangang, Taipei 11529, Taiwan.

[c] LIA (Associated International Laboratory), D3E (From Deep Earth to Extreme Events), Centre National de la Recherche Scientifique/Institut National des Sciences de l'Univers (France), Ministry of Science and Technology, Taiwan.

ABSTRACT - During the mid-Holocene, human groups from Taiwan migrated northeastward to the Ryukyu Islands, and southward to the Batanes Islands and Philippines. An important issue to understand these movements is whether the environmental conditions prevailing at present in the vicinity of Taiwan and in the South China Sea were already established at that time. Starting from the present-day situation, this paper describes the geomorphology, the wind patterns, and oceanic currents in the South China Sea, focusing on the region around Taiwan. In the context of conjunct Holocene sea-level rise and climate warming, it also characterizes the main forcing factors affecting climate variability during the last several thousand years. This paper thus reconstructs the likely sailing conditions during the mid-Holocene, at the time of the movement of the Austronesian-speaking populations from Taiwan and around the South China Sea. We suggest that El Niño Southern Oscillation variations may have played a significant role in reducing the strength of Kuroshio Current during El Niño events, offering more favorable sailing conditions for seafaring.

Keywords: Neolithic migrations; Austronesian-speaking people; Holocene climate; Western Pacific; South China Sea.

1. Introduction

Compared to the last glacial period ending around 11,700 years ago, the Holocene climate has been relatively warm and stable, allowing human populations to develop agricultural techniques and shift from nomadism to permanent settlements. During this period, groups of seafarers traveled long distances across the Pacific Ocean, potentially assisted by reversals in the direction of the trade winds associated with El Niño events (Anderson et al. 2006; Goodwin et al. 2014). Within this general context, the island of Taiwan is generally considered to be the main starting point of these extensive, middle to late Holocene human migrations (Bellwood 1997; Bellwood et al. 2007). The southward and

[1] Acknowledgements -This paper results from friendly discussions with Frank Muyard and Paola Calanca during 2013-2015 when Lionel Siame benefited from a delegation position at CNRS and was appointed as Visiting Associate Research Fellow at Institute of Earth Sciences, Academia Sinica (NSC 102-2811-M-001 and MOST 103-2811-M-001-135), and Adjunct Professor at National Central University (Earth Science Department). The editors, along with two anonymous reviewers, are sincerely acknowledged for their insightful comments and suggestions that helped improve our manuscript. We would also like to thank Pierre-Yves Manguin for his very helpful comments about Neolithic settlements in Taiwan and the sailing capabilities of Austronesians. This is contribution of the Institute of Earth Sciences, Academia Sinica, IESAS2373.

eastward movements of Austronesian languages-speaking populations (hereafter referred to as *Austronesians*) to the Philippines, Borneo, the Marianas, and Indonesia (between 4000 and 3000 years ago), and to Near Oceania and West Polynesia (starting 3300 BP), and then across East Polynesia (~1000 BP; Wilmshurst et al. 2011) have been explained by an expanding Neolithic demography and economy (Bellwood 2005, 2007; Diamond and Bellwood 2003) and key marine technology developments (Anderson 2005; Anderson et al. 2006).

Maritime conditions favoring long-distance seafaring depend largely on wind and surface current directions and strengths that fluctuate across seasonal and interannual timescales. Thus, any Holocene changes in seasonality and interannual climate variability, such as those associated with the El Niño Southern Oscillation (ENSO, see paragraph 2.4 for an explanation of this climatic phenomenon), may have shaped the opportunities Austronesians had to navigate out of Taiwan and around the South China Sea (SCS). Continuous records of such changes are notoriously difficult to extract from paleoclimate archives because these archives often lack the needed sub-annual resolution. However, recently published reviews compiling such data allows identification of periods of notable shifts in both seasonality and interannual variability during the Holocene, and indicate much reduced variability in the ENSO between 5000 and 3000 years ago (Emile-Geay et al., 2015).

One of the main objectives of this article is to describe the wind patterns and oceanic currents in the SCS, focusing on the Taiwan and Luzon straits (Figure 1), and to discuss the main sources of seasonal and interannual climate variability in these regions. Capitalizing on recent advances in the reconstruction of seasonality and ENSO activity during the Holocene, and in the context of conjunct Holocene sea-level rise, this article reviews the main forcing factors in climate variability during the last 10,000 years ago in the South China Sea and Taiwan regions. Finally, through comparison with archaeological evidence of Austronesian migrations such as pottery and jade artifacts, it highlights what may have been the main environmental factors shaping the routes used by Austronesian groups since the mid-Holocene around the SCS, and particularly to voyage from Taiwan.

2. The South China Sea: Present-day situation

2.1. Geomorphic context and bathymetry of the South China Sea

The SCS is the largest tropical marginal sea (a partially enclosed oceanic basin) in Southeast Asia (Figure 1). It extends from the equator to 23°N, from Singapore and the Indonesian archipelago to Taiwan and Luzon (Figure 1). Another characteristic of the SCS is the distribution of the surrounding reliefs, a key factor in the regional atmospheric patterns

across seasonal and interannual timescales. To the northwest and southwest, the bordering continent is mainly mountainous, particularly to the west. The Annamese Cordillera rises to roughly 2600 m and extends along the Vietnamese coast (Figure 1). To the south and to the east, the surrounding islands are also mountainous, with Mount Kinabalu in Borneo and Jade Mountain in Taiwan rising to ~4100 m and ~3950 m, respectively.

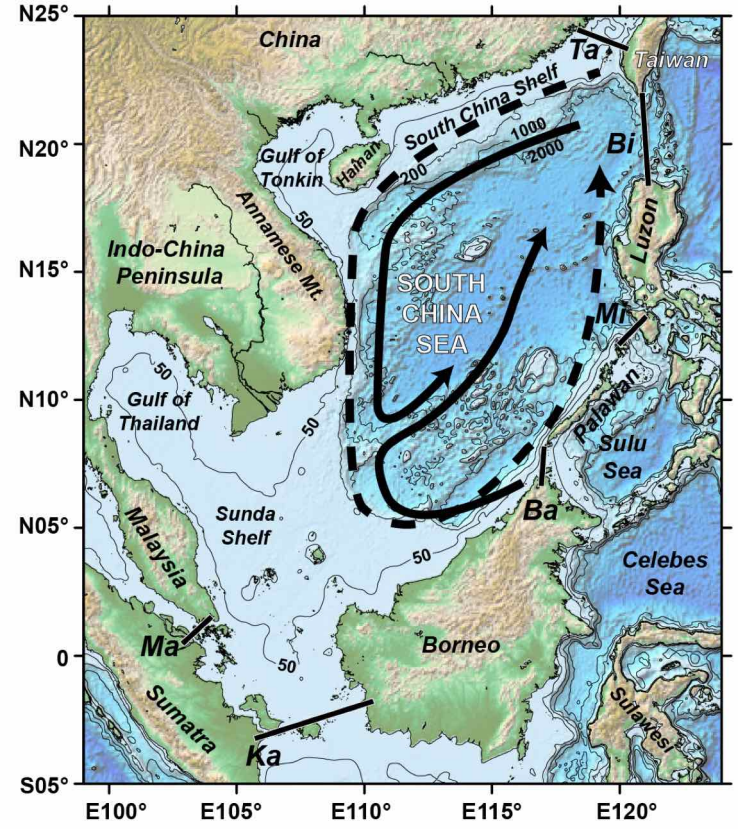

Figure 1 - Map of the South China Sea (SCS) region (modified after Wang et al., 2006, and Liu et al., 2002). Isobaths are given in meters below sea level (after Fang et al., 2006a). The SCS features seasonally alternating, basin-scale cyclonic gyres: the summer pattern (solid lines) involves a cyclonic gyre in the northern part and an anticyclonic gyre in the southern part. The winter pattern (dashed line) is characterized by a single cyclonic gyre affecting the entire basin. Solid black bars locate the different seaways allowing water exchanges between the SCS and the neighboring oceanic basins (maximum water depths after Wang and Li, 2009): B, Balabac Strait (~100 m); K, Karimata Strait (~50 m); L, Luzon Strait (~2400 m); Ma, Malacca Strait (~25 m); Mi, Mindoro Strait (~420 m); T, Taiwan Strait (~70 m). Abbreviations: Bat., Batanes islands; Yae., Yaeyama islands.

With an average depth of about 1140 m, the SCS bathymetry can be divided into three principal domains: the deep basin (15%), the continental slope (38%), and the continental shelf (47%) (Wang and Li 2009). Shallower than 100 m depth, continental shelves are wide along the northern and southwestern borders, whereas they are extremely narrow in the east and west (Figure 1). In the deepest parts of the SCS basin, the average water depth is on the order of 4700 m (Wang and Li 2009). Though at present the SCS is open on its northeastern and southwestern sides, it has been highly sensitive to sea level variations during previous glacial cycles since most of the bordering seaways are shallower than a few hundred meters (Figure 1). The SCS is connected to the Philippines Sea (Pacific Ocean) by the Luzon Strait (~2400 m) and to the Sulu Sea thanks to both the Mindoro (~420 m) and the Balabac (~100 m) straits (Figure 1). The southern connection with the Indian Ocean (through Karimata and Malacca straits) is also relatively shallow and only limited by the depth of the continental shelf. While the deepest part of the SCS basin may exceed 5000 m, exchanges of water with

other bordering seas below a few hundred meters primarily occurred through the Luzon Strait during low sea level periods such as the Last Glacial Maximum (LGM).

2.2. Atmospheric circulation over the South China Sea

Because the SCS is located between the Asian continental landmass (South China and Indochina Peninsula) to the west and the Pacific Ocean to the east, it plays a major role in the formation of the Southeast and East Asian monsoons. Impacting all the neighboring countries, the monsoon regime is a seasonal, planetary-scale climatological phenomenon linked to the differential heating between landmasses and oceans and the resulting pressure gradient, combined with the swirl introduced to the winds by the Earth's rotation (see An et al. 2015, for a recent review). Primarily regulated by atmospheric and oceanic cross-equatorial heat transport, the Southeast and East Asian monsoons are driven by the thermal differences between the Asian landmass and the Pacific Ocean (An 2000; An et al. 2015).

To the northwest of the monsoon front (Figure 2), continental Asia is strongly influenced by the dry Siberian High[2], which is subject to large seasonal temperature variations (Wu and Wang, 2002). Conversely, to the southeast of this front, the weather of the Asian coastal regions is controlled by moisture-laden air mass originating from the Pacific (An et al. 2015). The summer is typically a rainy season, whereas the winter monsoon is drier (Figure 2). During summer, continental Asia heating induces a low-pressure area that brings heavy rainfalls above the continent. During winter, this system is reversed with the cooling of the landmass triggering a high-pressure system and pushing cool and dry air over the ocean (Figure 2). Because the seasonal variability of the temperature is larger over the landmass than over the ocean, the temperature gradient yields a surface-air pressure gradient that seasonally changes its direction, and in turn triggers NW and SE surface winds in winter and summer, respectively (An et al. 2015). In September, the winds are dominated by the Southwest monsoon, with the Northeast monsoon appearing in the northern part of the SCS (above roughly 20°N), while the Southwest monsoon is still prevailing in its southern part. From October to November, the Northeast monsoon expands gradually to the south and reaches its maximum strength and cover in December. The winter monsoon generally ends in

[2] The Siberian High is a high pressure zone that forms during a significant part of the year over Siberia, usually centered on Lake Baikal. During the winter, it is the largest in size and pressure of all the anticyclonic zones of the northern hemisphere.

April. The summer monsoon starts again in May, culminating during July and August and affecting the whole SCS region.

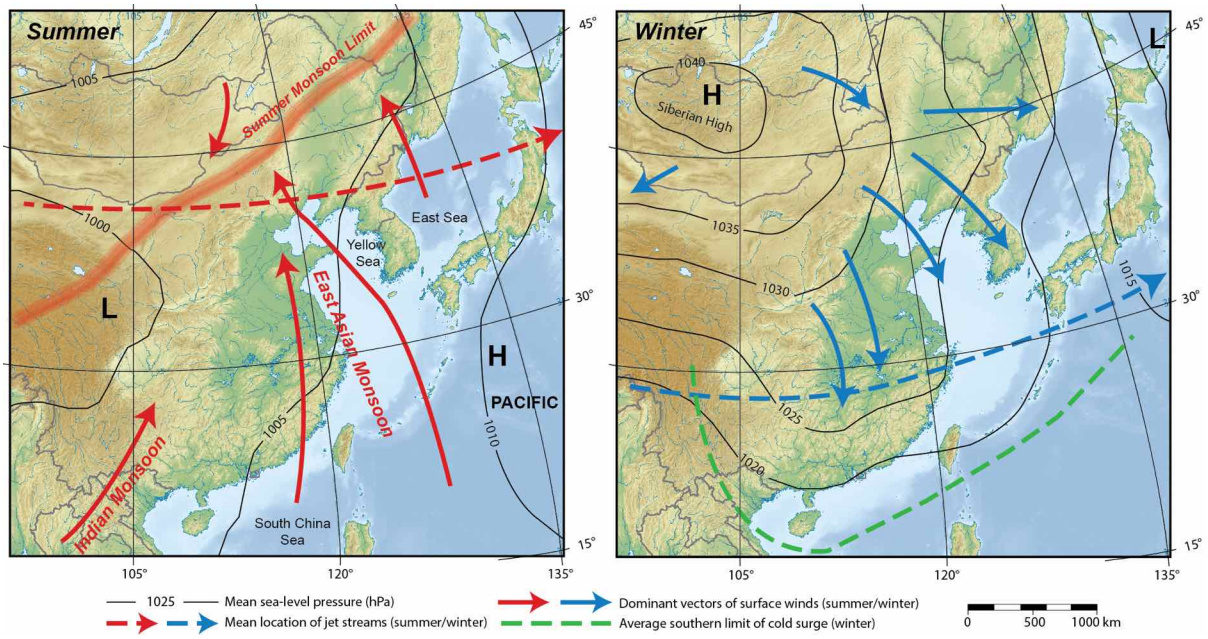

Figure 2 - Schematic maps of the seasonal changes in the wind system of East Asian monsoon region (modified after Yi, 2011).

2.3. Oceanic circulation within the South China Sea

In the South China Sea, the oceanic circulation is driven by the seasonally changing monsoon winds and channeled by the geographic distribution of the coastlines (Shaw and Chao, 1994). In particular, the Indochina Peninsula and the mountainous relief of Southern China block the landward summer monsoon winds and produce a wind jet, which in turn triggers surface currents that are roughly parallel to the NE-SW long axis of the SCS basin (Xie et al. 2003; Liu et al. 2004). At the basin scale, the strong orographic control over surface winds is thus responsible for an alternating system of oceanic gyres (Figure 3). The summer pattern involves a cyclonic gyre in the northern part and an anticyclonic gyre in the southern part, whereas the winter system is characterized by a single cyclonic gyre affecting the whole basin (Shaw and Chao 1994; Hu et al. 2000; Xue et al. 2004; Liu et al. 2002; Wang et al. 2006). During the Northeast winter monsoon, the combination of the wind-triggered and strong gradient forcing results in a southwestward and southward coastal current system off the coasts of China and Vietnam (Figure 3). In the summer, during the Southwest monsoon, these coastal currents are reversed and flow northeastward (Figure 3).

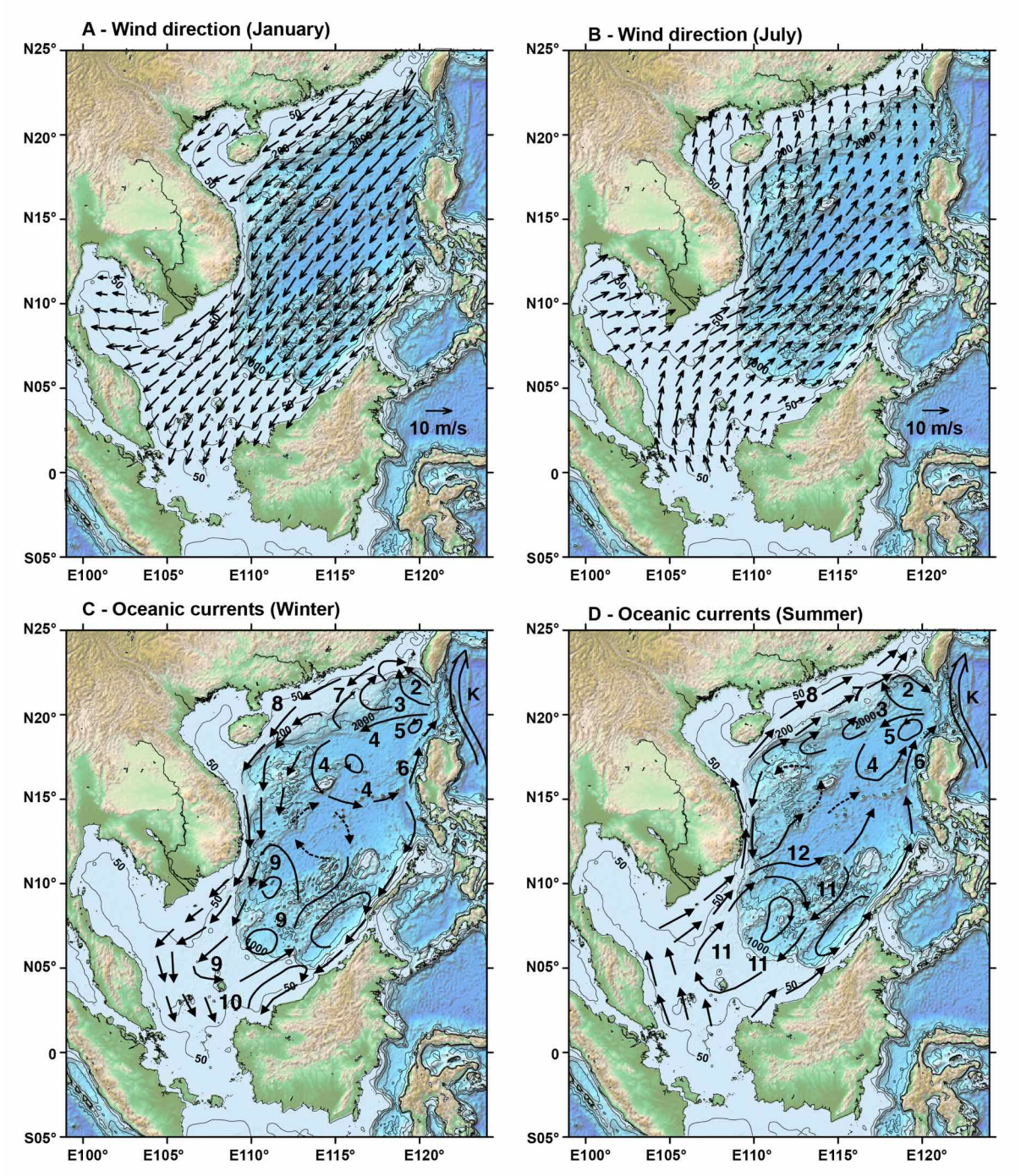

Figure 3 - Climatological mean field of the surface winds during 1993-2003 for (A) January and (B) July (modified after Fang et al., 2006a) and surface circulation of the modern South China Sea showing opposite patterns between (C) winter and (D) summer (modified after Fang et al., 2006a). Keys: K, Kuroshio main current; 2, Kuroshio current loop in SCS; 3, South China Sea branch of Kuroshio; 4, Luzon cyclonic gyre; 5, Luzon cyclonic eddy; 6, Luzon coastal current; 7, SCS Warm Current; 8, Guangdong coastal current; 9, SCS southern cyclonic gyre; 10, Natuna off shelf current; 11, SCS southern anticyclonic gyre; 12 Vietnam offshore current.

2.4. Interannual variability, the role of the ENSO

Interannual variability of atmosphere and ocean dynamics associated with the ENSO are superimposed on the first-order seasonal mode of the SCS variability (Fang et al. 2006b). This has repercussions for the monsoon dynamics (Webster et al. 1998). El Niño events, and their La Niña counterparts, are large-scale equatorial meteorological phenomena that affect wind systems, sea surface temperatures, and precipitation in the tropical Pacific Ocean. They correspond to two opposed phases of a coupled ocean/atmosphere system, and have an important impact on the global Earth's climate. In a normal situation (ENSO-neutral phase), trade winds blow from east to west on both sides of the equator, driving the surface waters warmer than 27°C to pile-up in the western tropical Pacific basin over a thickness of about 100 meters (Figure 4). The resulting Indo-Pacific warm pool is responsible for strong evaporation and deep atmospheric convection at the origin of intense rainfalls. In turn, the upwelling of cold and nutrient-rich waters along the coast of Peru and the equatorial divergence that feed the eastern equatorial Pacific sustains a zonal sea surface temperature gradient along the equator in the Pacific Ocean (Kessler 2006). Above the eastern equatorial Pacific, a descending dry air mass feeds eastern trade winds blowing along the equator. The zonal atmospheric loop involving basin-scale atmospheric circulation in the troposphere is known as the Walker circulation (Figure 4), and is altered every two to seven years when major ocean-atmosphere reorganizations in the tropical Pacific region occur during El Niño years (Rasmusson and Carpenter 1982).

At the early beginning of an El Niño event, the weakening of the trade winds is generally associated with several westerly wind bursts blowing above the western Pacific warm pool that can last a few weeks, initiating strong eastward-flowing warm currents (Rasmusson and Carpenter 1982; McPhaden 2015). These eastward-flowing warm currents in turn feed back to the atmosphere, initiating a westward drift of the deep atmospheric convection and its associated rainfall that closely track the warm oceanic temperatures (Figure 4). If this situation is maintained long enough, it can lead to an El Niño event (Rasmusson and Carpenter 1982; McPhaden 2015). Dry conditions then develop over South-East Asia and Australia (producing forest fires), tropical storms and cyclones appear much farther east than usual, affecting the Polynesian Islands, while the western coasts of South America experience unusual rainfall causing floods and landslides. In addition, fish populations dramatically decrease within the coastal waters of South America, the warm waters being much poorer in nutrients than the usual upwelling of deeper, cold waters. El

Niño episodes usually begin in mid-year, last from 6 to 18 months, and reach their maximum intensity around the end of December (Rasmusson and Carpenter 1982).

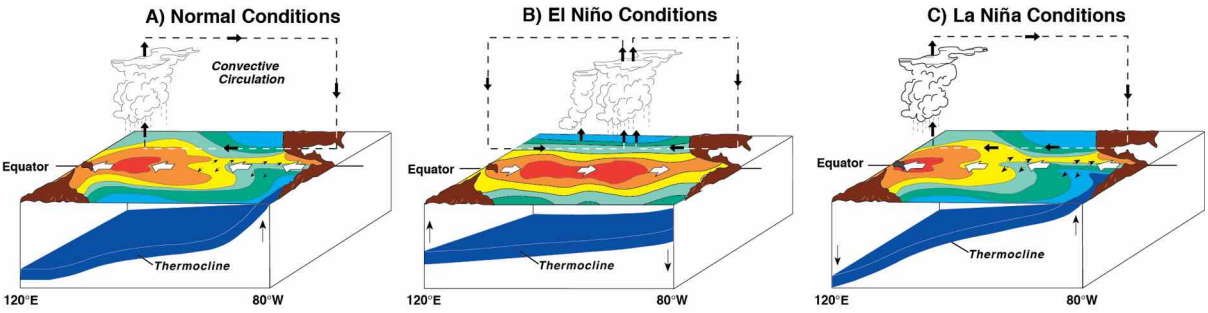

Figure 4 - Sketch diagrams showing the three main phases of the ENSO phenomenon (source: NOAA/PMEL/TAO http://www.pmel.noaa.gov/tao/proj_over/diagrams/index.html). A: Normal Pacific pattern: Equatorial winds gather warm water pool toward the West. Cold water upwells along South American coast. B: El Niño conditions: Warm water pool approaches the South American coast. The absence of cold upwelling increases warming. C: La Niña conditions: Warm water is farther west than usual.

In terms of air-sea heat exchange, the SCS can be regarded as a relatively well-balanced system: heat is released to the atmosphere in the northern basin through evaporation during the Northeast monsoon in fall and winter, while the ocean accumulates heat in the southern basin due to excess insolation in spring and summer (Chao et al. 1996). When averaged over the year, these processes tend to balance one another.

El Niño events perturb the SCS on an interannual time scale. For example, surface winds over the SCS exhibited anticyclonic anomalies during recent El Niño events (1994-1995, 1997-1998, 2002-2003) and cyclonic anomalies during La Niña events (1995-1996; 1998-2000) (Fang et al. 2006a; Liang et al. 2000). Wang et al. (2000) reported that anomalous anticyclones (cyclones) were present in the northwestern Pacific during such warm (cold) events. Fang et al. (2006a) also observed that the Northeast monsoon weakens (intensifies) during the ENSO warm (cold) phase over the Northern SCS, including the Taiwan and Luzon Straits, whereas this is not the case over the Southern SCS. The winter cyclonic circulation is reduced during El Niño periods, which is a result of the anticyclonic anomaly of the wind stress (Wang et al. 2006). During El Niño events, sea surface temperature elevation indicates a basin-wide warming of the entire SCS, which occurs with a lagged response of about 8 months, sometimes attributed to the weakening of the Northeast monsoon over Taiwan and Luzon regions (Fang et al. 2006a). In 1998, this weakened

Northeast monsoon brought less cold and dry air to the atmosphere over the SCS, and induced weaker southwestward cold current toward the SCS (Wang et al. 2006).

2.5. Ocean and atmosphere circulations around Taiwan

The North Equatorial Current (NEC) flowing north of the equator within the Pacific Ocean reaches the Philippine Archipelago along the eastern coast of Luzon and splits into two branches: one southward-flowing branch giving birth to the Mindanao Current, and one northward-flowing branch forming the Kuroshio Current. Between Luzon and Taiwan, the Kuroshio Current marks a slight excursion within the Luzon Strait (Figure 3), exchanging deep waters with the northern SCS and then resuming its northward course along the eastern coast of Taiwan (Shaw and Chao 1994; Hu et al. 2000; Centurioni et al. 2004; Xue et al. 2004). Further to the north, the Kuroshio Current flows along the Okinawa Trough and the eastern Japanese coastlines before merging with the southward-flowing Oyashio Current and flowing back eastward at mid-latitudes where it becomes the North Pacific Current (Hu et al. 2015).

Taiwan Island is bounded by the Taiwan Strait to the west, the Pacific Ocean to the east, the East China Sea to the north and by both the SCS and the Luzon Strait to the south (Figure 1). On both sides of the Taiwan Strait, the combination of mountainous relief of China (with an average elevation of about 500 m) and of the north-trending mountain belt of Taiwan (peaking at 3950 m) induce a strong wind jet during the Northeast monsoon (winter) through wind canalization process (Zhang 1997). At the level of the Taiwan Mountains, the weak winds in the wake and the strong winds along the eastern side result in accelerated winds at the southern tip of the island (Liu and Xie 1999; Wang et al. 2008; Deng et al. 2012). This well-established orographic forcing leads to a strong south-trending coastal drift current along the eastern coast of Taiwan during winter. In the Northern SCS, the blockage of the Northeast monsoon winds by the mountains of Taiwan and the relief of Luzon also drives strong wind curl dipoles, which in turn induce alternating clusters of cyclonic and anticyclonic eddies (Wang et al. 2008).

During summer, a northward current triggered by the summer monsoon winds dominates the Taiwan Strait (Hu et al. 2010). The wintertime current pattern has long been more controversial (Qiu et al. 2011 and references therein). To solve this issue, Qiu et al. (2011) used the trajectories of satellite-tracked surface drifters, deciphering the near surface circulation in the Taiwan Strait. Unlike many previous studies that proposed a northward

(southward) current prevailing in the eastern (western) part of the Taiwan Strait, this study showed that all the drifters that entered the Taiwan Strait during winter eventually moved southward after passing the Penghu Islands. This permitted identification of three current patterns: (1) a "through-flow" trajectory that enters the SCS flowing westward along the Chinese continental slope, (2) a loop current that circulates anti-cyclonically and returns to the Kuroshio Current east of Taiwan, and (3) a "blocked" intrusion that penetrates into the Taiwan Strait without being able to go further north than the Penghu Archipelago (Figure 5).

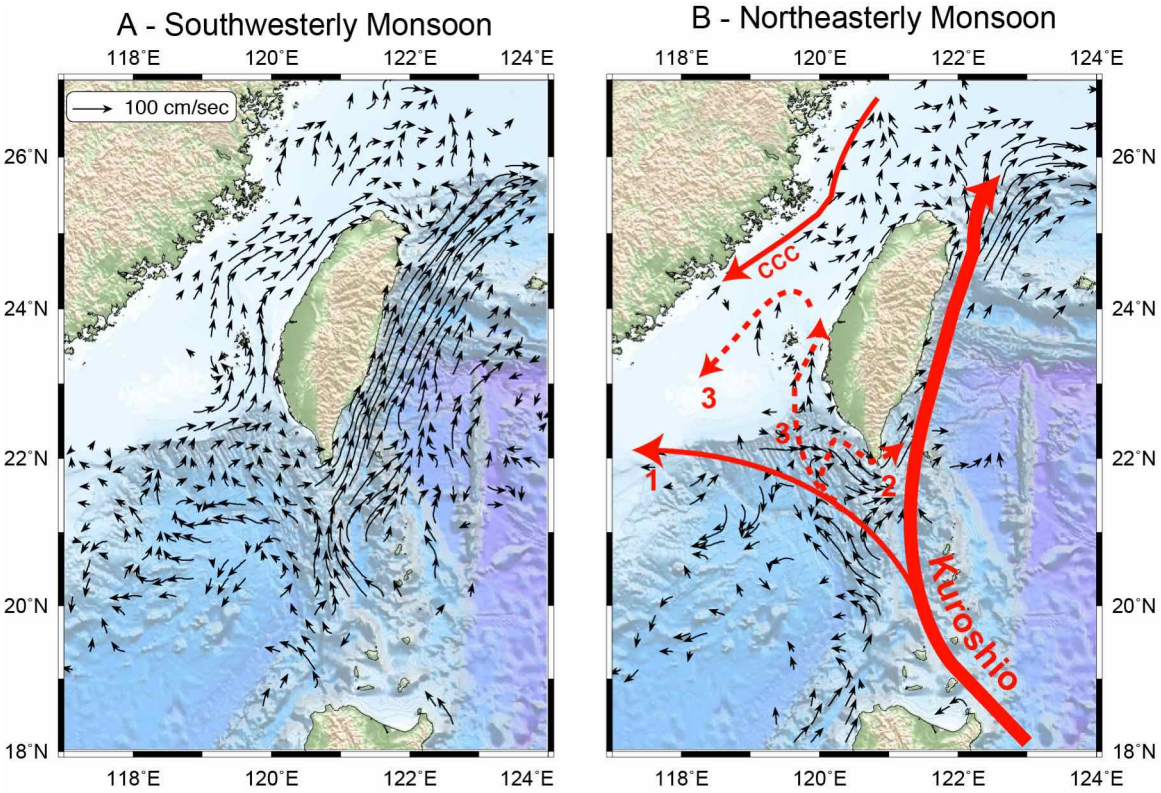

Figure 5 - Current velocity vectors (at 30 m depth) measured by shipboard acoustic Doppler current profiler during 1991-2000 at 30 m around Taiwan (modified after Liang et al., 2000), shown for seasons of southwesterly monsoon (summer, left) and northeasterly monsoon (winter, right). On the right panel, the arrows show the schematic diagram of near-surface circulation around the Taiwan Strait in winter as observed by surface drifters during 1989-2007 (after Qiu et al., 2011). Keys: 1, " Through-flow " trajectory; 2, Loop current; 3, " Blocked " intrusion; CCC, China Coastal Current.

3. The South China Sea during the Holocene

3.1. Sea level variability

During the LGM, which peaked some 21,000 years ago, the global average sea level was about 120 m lower than the present day, and large amounts of water were stored in expanded ice sheets in the northern hemisphere. At this time, the isolation and connectivity of

islands and archipelagos were much different than their modern-day configurations, having a profound impact on the regional paleogeography and accessible landmasses (Wallace and Woodroffe 2014). Around the South China Sea, emerged continental shelves and extended continental surfaces, which introduced oceanic circulations different from modern conditions. Since the SCS was almost enclosed, exchanges of seawater with the Pacific Ocean occurred exclusively through the Luzon and Mindoro straits (Figure 1). To the South, the SCS basin was bordered by the emerged Sunda-Sahul platform that comprised the Indonesian archipelago as well as the Australia-New Guinea landmass. This wide continental area must have altered the heat balance of the region by blocking the warm oceanic current due to the closure of the Torres Strait between Australia and Papua-New Guinea (DiNezio and Tierney 2013). To the south, the closed seaways within the Indonesian archipelago also led to a cessation of the Leeuwin current and a decrease in sea surface temperatures along the western coast of Australia (Wells and Wells 1994; Kutzbach and Guetter 1986). To the north, the SCS basin was limited by the South China Shelf, which bridged Taiwan to the Asian mainland thanks to the closure of the Taiwan Strait (Figure 6).

In East Asia, the early part of the Holocene was characterized by increasing sea surface temperature (Leduc et al. 2010) and a rapid rise in relative sea level that occurred between 9,500 and 8,500 BP and culminated in the middle Holocene (Tjallingii et al. 2010; Nunn and Carson 2015). In the western Pacific regions, like the Philippines, sea level was 3 m higher during the period from 6,000 to 4,100 years ago before declining to the present situation (Berdin et al. 2003; Maeda et al. 2004). In Taiwan, the relative sea level reconstruction during the Holocene both relies on regional and local proxies (Hsieh et al. 2004). Prior to 11,000 BP, it is generally assumed that it was equivalent to that of the Sunda Shelf (Chen and Liu 2000), one of the most reliable sea level records ever documented (Hanebuth et al., 2000). From the LGM to 15,000 BP, the sea level curve suggests an average rate of sea level rise of about 3 mm/yr (Figure 6). During the *Melt-water Pulse 1A*[3] (Fairbanks 1989; 15,000-13,500 BP), the sea level may eventually have risen at a rate greater than 20 mm/yr, finally decreasing to 8-9 mm/yr during the period 13,500-11,000 BP (Figure 6). To determine the sea level datum and its associated uncertainties at about 11,000-10,000 BP (Figure 6), Hsieh et al. (2004) directly connected the curve from the Sunda Shelf to that constructed by Chen and Liu (2000). They thus estimated that the rate of sea level rise might have been on the

[3] Meltwater pulse 1A is an abrupt acceleration of the sea-level rise that occurred 14,600 years ago during the last deglaciation. During this short period, sea level rise greatly exceeded the speed at which sea level rose before and after this anomaly.

order of 18 mm/yr, which could be correlated to the *Melt-water Pulse 1B* described in Fairbanks (1989). For 10,000 and 6,000 BP, Chen and Liu (2000) averaged sea levels reported elsewhere around the Pacific and estimated for Taiwan display values of -30±7 m and -2±4 m, respectively. The last part of the curve (4,800 BP to now) relies on the dating of coral platforms in the Penghu Islands (Chen and Liu, 1996). During this period, the sea level fell gradually from its maximum of about +2.3 m to the modern sea level (Figure 6).

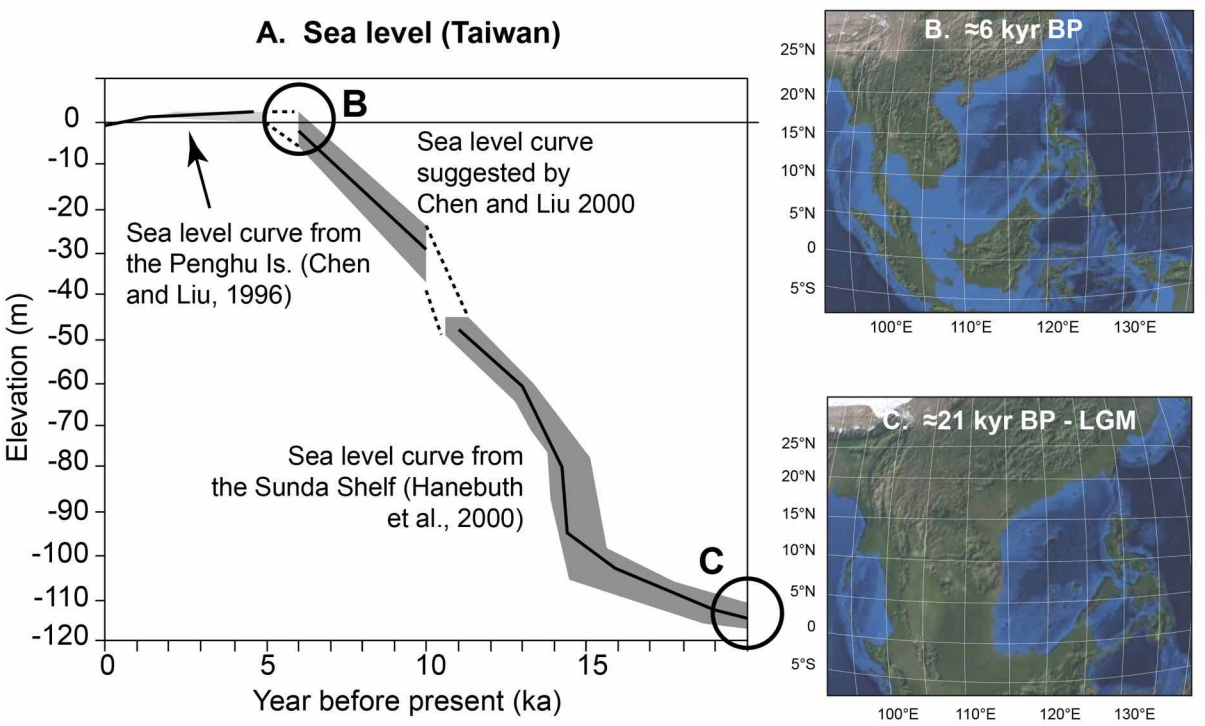

Figure 6 - A. Relative sea level curve for Taiwan during the last 20 kyr (after Hsieh et al., 2004). B and C. Schematic representations of the coastlines around the South China Sea at ~21 kyr and ~6 kyr, respectively (after Bluemarble 3000 by Meyer and Rege, 2011).

3.2. Holocene changes in the tropical atmospheric variability, the ENSO and the Kuroshio Current

During the Holocene, the Pacific Ocean experienced large-scale atmospheric changes, mainly triggered by modifications of key climate boundary conditions such as Earth's orbital parameters. In particular, shifts in seasonal solar radiation caused by Earth's precession may have forced the intertropical convergence zone (ITCZ) to move southward to its present-day position (Haug et al. 2001; Abram et al. 2009). These changes in seasonal insolation led to a gradual weakening of the Asian monsoon during the last 10,000 years ago (Wyrwoll and Miller 2001; Wang et al. 2000; Wang et al. 2005; Yancheva et al. 2007), a feature that affected the seasonal hydrological parameters in the SCS (Yokoyama et al. 2011). Further to the south, stalagmites from Borneo indicate that precipitation maxima occurred at ~5,000

years ago, *i.e.,* a few millennia later than for the date for speleothems from China (Partin et al. 2007). In the southern part of the Indonesian archipelago, a Holocene reinforcement of the summer monsoon mirrors the decay of the East Asian monsoon (Mohtadi et al. 2011), as would be expected if the southward migration of the ITCZ were involved in the evolution of the western tropical Pacific hydro-climate during the Holocene. Those large-scale changes in the atmospheric circulation induced by a southward migration in the ITCZ driven by orbital parameters altered at first-order the tropical Pacific hydro-climate through changes in rainfall seasonality.

Contrasting with this broad picture, the Holocene evolution of ENSO at interannual timescales is still poorly understood. This is caused by (1) interfering multiple climatic forcing factors that alter the ENSO, and (2) the difficulty of retrieving reliable records of interannual climatic variability within the tropical Pacific area. During the last 10,000 years, ENSO variability was first believed to have increased from a relatively weak level in the early to mid-Holocene to its modern strength (Tudhope et al. 2001; Moy et al. 2002; Koutavas et al. 2006; Leduc et al. 2009). This view persisted for more than a decade, and was consistent with modeling experiments since virtually all the ocean-atmosphere general circulation models forced by orbital parameters simulate a reduction of ENSO activity during the early and mid Holocene, along with a strong reduction in the annual cycle of the eastern equatorial Pacific (Clement et al. 1999; Emile-Geay et al. 2007; Brown et al. 2008; Phipps and Brown 2010; Masson-Delmotte et al. 2013). Liu et al. (2000) suggested that El Niño in the Early Holocene was reduced at least in part by the remote influence of the intensified Asian monsoon on the Pacific trades. Later data (Marchitto et al. 2010; Zhang et al. 2014) suggested that solar activity may have controlled centennial-scale changes in ENSO to some extent.

Recently, a series of new ENSO reconstructions have revised the paradigm of a gradual ENSO increase during the Holocene. These indicate (1) significant millennial-scale changes in ENSO activity during the early Holocene (Marchitto et al. 2010; Cobb et al. 2013; Carré et al. 2014; Zhang et al. 2014; Emile-Geay et al. 2015), muted ENSO activity during the mid-Holocene (Conroy et al. 2008; Cobb et al. 2013; McGregor et al. 2013; Zhang et al. 2014; Carré et al. 2014; Emile-Geay et al. 2015; Chen et al. 2016) and (2) a rapid ENSO reinvigoration dated between 4,000 and 3,000 years ago (Conroy et al. 2008; Cobb et al. 2013; Zhang et al. 2014; Emile-Geay et al. 2015).

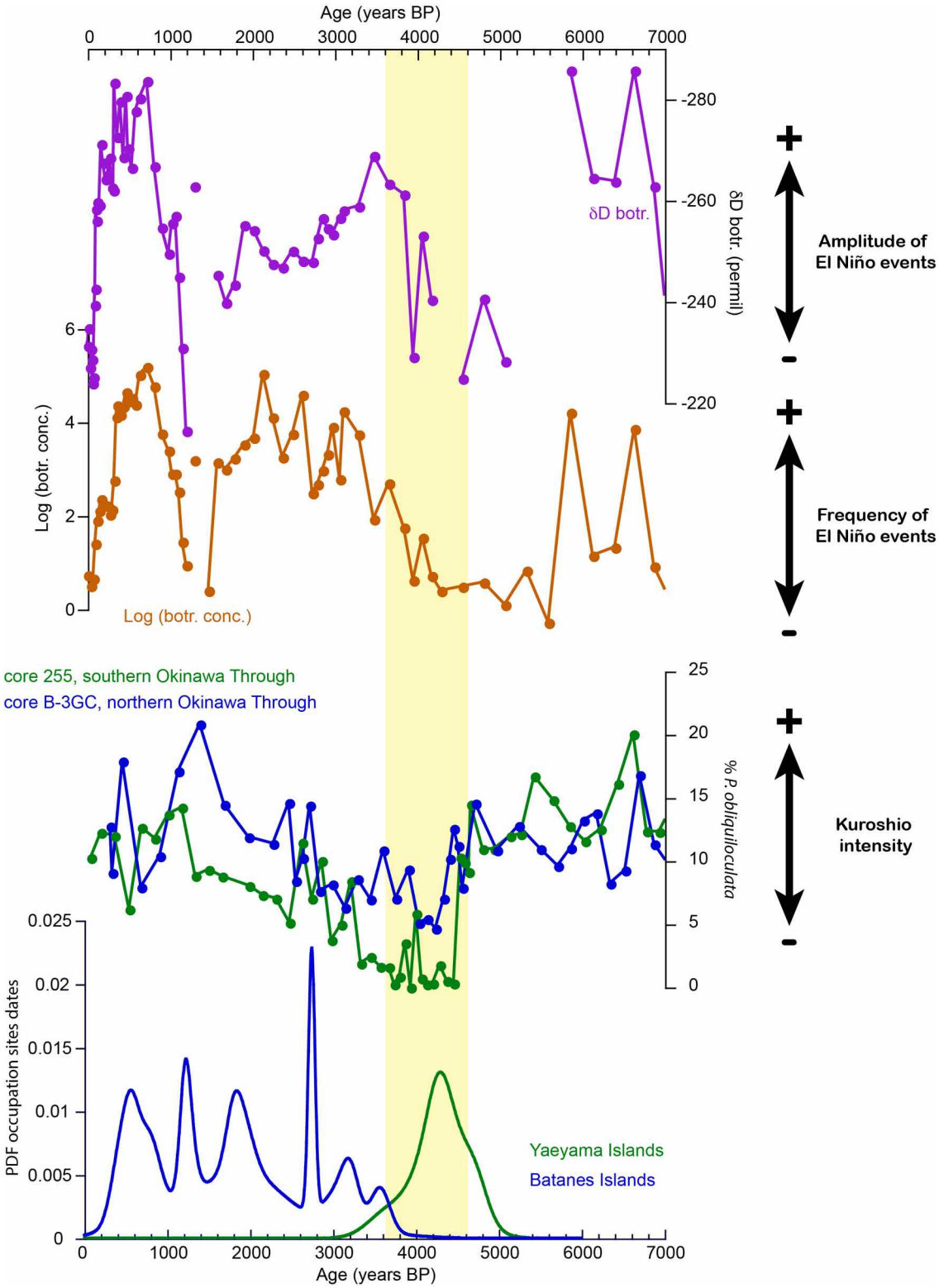

Figure 7 - A. Holocene sedimentary records from El Junco Lake, Galapagos, used as proxies for El Niño amplitude (δD measured on botryococcenes, in purple) and frequency (botryococcenes concentrations plotted on a logarithmic scale) (Zhang et al., 2014). B. Holocene sedimentary records from northern (blue curve) and southern (green curve) Okinawa Trough, illustrating the abundance of the planktonic foraminifera *Pulleniatina obliquiloculata*, indicative of the Kuroshio Current (Jian et al., 2000). C. Probability density functions (PDF) of archeological dates reported for the Yaeyama Islands, east of Taiwan (green curve, Summerhayes and Anderson, 2009; Hudson, 2017) and the Batanes Islands, north of Luzon (blue curve, Anderson, 2005; Bellwood and Dizon, 2013).

Interestingly, the above-mentioned timings for ENSO changes in its modes of operation during the Holocene are analogous to those experienced by the Kuroshio Current strength as evidenced in marine sediments collected from the Okinawa Trough (Jian et al., 2000; Ujiié et al., 2003). In particular, two different and independent reconstructions of the Kuroshio Current strength indicate an abrupt decrease of its intensity between 4,500 and 2,500 years ago, coinciding with a rapid increase in ENSO amplitude and frequency (Jian et al. 2000). This led Ujiié et al. (2003) to suggest that the decreased strength of the Kuroshio Current observed during the mid-Holocene to late Holocene in the Okinawa Trough was associated with a reinvigoration of ENSO (Figure 7).

4. Discussion

Pleistocene glaciations lowered the sea level by roughly 120 m in the Taiwan Strait, bridging Taiwan to the Asian mainland. Paleolithic artifacts along the coast of China and in Taiwan attest to human settlements on both sides of this land bridge (Chang 1989). After the LGM, the Taiwan Strait formed relatively quickly as the sea level rose, with a complete separation of Taiwan from the mainland at about 8,000 BP (Figure 6). In Taiwan, the transition from cold-dry to warm-wet conditions that occurred since the LGM is evidenced by a large increase in the tree/herb ratio observed in continental records (Liew et al. 1998; Wei 2002), with increasing warm and wet conditions after 11,000 BP and a clear climatic optimum from 10,000 to 7,000 BP (Liew et al. 2006a, 2006b). These paleo-climate proxies are in good agreement with cosmogenic exposure dating of glacial morphologies preserved in the Central Mountain Range of Taiwan (Nanhutashan), demonstrating the disappearance of high elevation, glacier-friendly conditions after 9,000-8,000 BP (Siame et al. 2007) in conjunction with the drastic reduction of the winter monsoon and a strong summer monsoon induced by a northward migration of the ITCZ during the early mid-Holocene (Huang et al. 1997; Yancheva et al. 2007). A rising sea level is probably the major environmental change experienced by the SCS region during the last 15,000 years. According to several studies (Lape et al. 2007; O'Connor 2007; Erlandsson 2010; O'Connell et al. 2010), archaeological evidence also indicates that non-Austronesian groups from insular Southeast Asia were already mastering seafaring techniques some 30,000 years ago (Madhi 2013). After the LGM, flooding of the Sunda-Sahul shelf must have forced those populations to migrate on continental areas.

In Taiwan, the first pottery-making Neolithic cultures appear around 5,500 ago, with human groups coming from what is now South China (Anderson 2005). By 4,500 to 3,900 years ago (Summerhayes and Anderson 2009; Hudson 2017) and around 4,000 BP (Bellwood and Dizon 2013), migrations to the southern Ryukyu (Yaeyama) and Luzon/Batanes Islands occurred, respectively (Figure 7). The reason why settlements in the Yaeyama islands did not last after 3,900 BP is beyond the scope of this paper. However, in addition to the probable difficulties in beating against the Kuroshio Current on the way back to Taiwan, the Yaeyama Islands are also prone to destructive tsunamis (Goto et al. 2010; Nakamura 2006). Such catastrophic events may have affected the human population that settled on their shores. For example, in 1771, the Meiwa tsunami, with a height of roughly 30 m above sea level, attacked the east coast of Ishigaki and killed almost the entire population.

Taiwan is separated from northern Luzon by a 350 km wide stretch of water, with small but habitable islands (Figure 1). The Luzon Strait tends to have rough seas and very windy weather, especially under the Northeast winter monsoon. Though it can generate southward surface counter-currents, the dominant and permanent Kuroshio Current set along the eastern Philippines, and northeast Taiwanese coasts, flows northward all year round. If this major oceanic current were favorable to sailing from Taiwan to the southern Ryukyu Islands (Summerhayes and Anderson 2009), it would have made maritime movement from Taiwan to the Batanes Islands and northern Philippines very difficult. Considering only the surface winds, the best period to sail southward from Taiwan to Luzon appears to be during the boreal winter, in the lee of Northeasterlies. From that perspective, the experience of Qiu et al. (2011) using satellite-tracked surface drifters is instructive. During that particular season, the drifters released within the Luzon Strait show tracks that either go westward following the slope of the Asian continental platform, become trapped by the current loop linked to the Kuroshio Current intrusion into the Luzon Strait and then follow the Kuroshio Current along the eastern coast of Taiwan, or eventually enter the Taiwan Strait to the Penghu Islands (Figure 5). Not a single drifter followed a southward route towards the Batanes and/or Luzon Islands. This important observation suggests that even if winter conditions intuitively appear more favorable than those prevailing during summer, Austronesians would still have to travel against the Kuroshio Current, and probably need strong sailing capabilities to beat against the wind and northward currents.

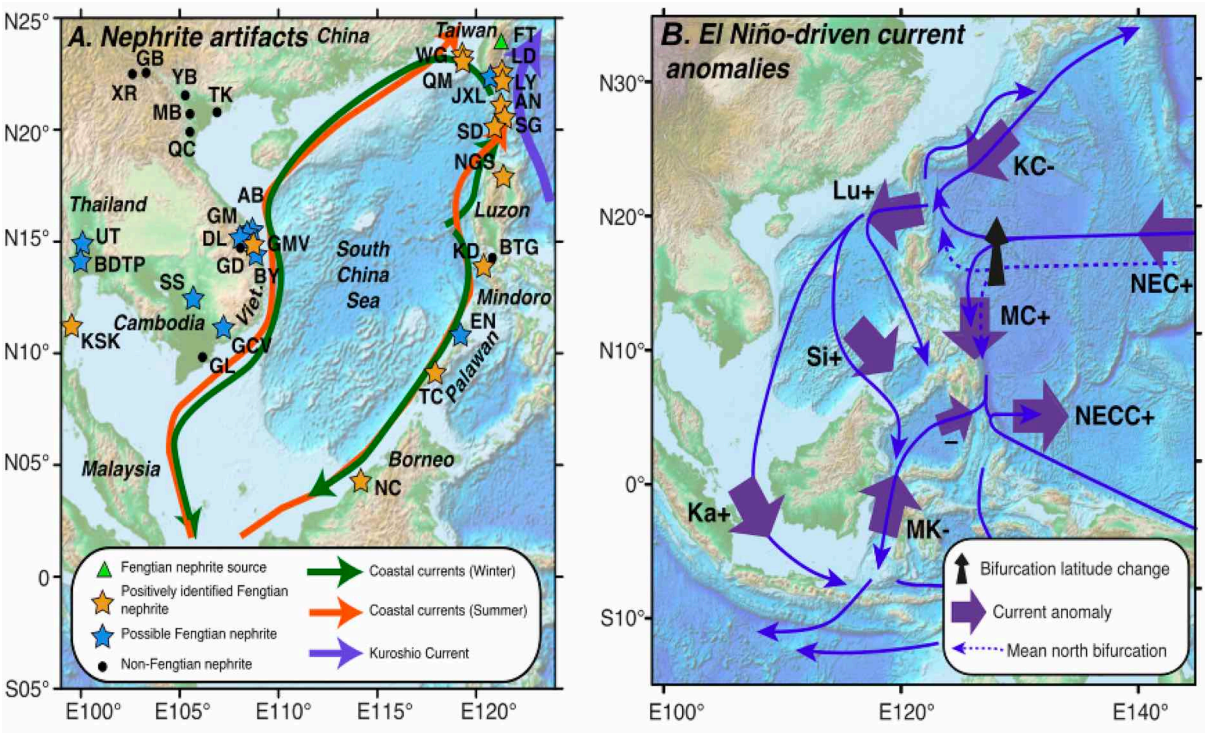

Figure 8 - A. Distribution of Taiwan nephrite artifacts in Southeast Asia, 5000 BP-500 AD (after Hung et al. 2007) together with winter (green arrows) and summer (orange arrows) coastal currents around the SCS (simplified from Fang et al. 2006a). Keys: green triangle, Fengtian nephrite deposit in Taiwan; Yellow stars, sites outside Taiwan with positively identified Fengtian nephrite artifacts; Blue stars, sites with jade artifacts of possible Fengtian origin; Black circles, sites that have identified nephrite of non-Fengtian origin. Geographic names: WG, Liyushan, Wangan Islands; QM, Nangang, Qimei Islands, Penghu Archipelago; JXL, Jialulan, eastern Taiwan; LD, Yugang and Guanyindong, Ludao Islands; LY, Lanyu High School Site, Lanyu Islands; AN, Anaro, Itbayat Islands; SG, Sunget, Batan Islands; SD, Savidug, Sabtang Islands; NGS, Nagsabaran, Cagayan Valley; KD, Kay Daing, Batangas; EN, Leta-Leta and Ille Caves, El Nido, Palawan; TC, Tabon Caves, Palawan; NC, Niah Cave West Mouth, Sarawak; AB, An Bang; GM, Go Mun; DL, Dai Lanh; GMV, Go Ma Voi; BY, Binh Yen; GCV, Giong Ca Vo, Ho Chi Minh City; SS, Samrong Sen, Cambodia; UT, U-Thong, Suphanburi; BTDP, Ban Don Ta Phet, Kanchanaburi; KSK, Khao Sam Kaeo, Chumphon; BTG, Uilang Bundok and Pila, Batangas; TK, Trang Kenh; YB, Yen Bac; MB, Man Bac; QC, Quy Chu; GB, Go Bong; XR, Xom Ren; GD, Go Dua; GL, Giong Lon. B. Impact of El Niño on the Pacific Western Boundary Currents (modified after Hu et al. 2015). During the developing phase of an El Niño until three to four months preceding the climax, the Kuroshio Current decreases while the Mindanao Current increases. Keys: minus (-) and plus (+) refer to current decrease and increase, respectively. Abbreviations: Ka, Karimata; Si, Sibulu; Lu, Luzon; KC, Kuroshio Current; MC, Mindanao Current; NEC, North Equatorial Current; NECC, North Equatorial Counter Current.

Comparing paleoclimate proxies with archaeological or historical records is challenging. Indeed, even if great progress has been achieved during the last two decades (Caseldine and Turney, 2010), there remain many sources of uncertainty in attempting to firmly assign the evolution of a given civilization to a climate change. With no major sea level changes after 6,000-5,000 BP (Behre, 2003), the large-scale oceanic circulations were already established in the SCS basin and surrounding oceanic basins at that time. Yet, interannual alterations of those oceanic and atmospheric patterns able to alleviate the difficult

sailing conditions may have offered opportunities to sail out of Taiwan. Such ENSO-related environmental influences are indeed thought to have impacted human societies in the tropical Pacific Ocean, driving significant societal changes (Allen 2006) or even assisting long distance voyaging in the conquest of the far East Pacific (Anderson et al. 2006; Goodwin et al., 2014; Montenegro et al. 2016). In the case of the Taiwan region, ENSO-like events tend to weaken the winter monsoons. Thus, during El Niño events, seafaring conditions from Taiwan to Luzon may have thus been a little less unfavorable, helping Austronesian groups to reach Luzon and then the Batanes Islands (Anderson 2005; Hung et al. 2007), which are easier to access directly from Luzon under normal sailing conditions (Figure 3). Comparison of archeological dates in the Yaeyama (4,500-3,900 BP), and Batanes/Luzon (4,000-3,000 BP) islands with paleoclimate indicators of ENSO amplitude and intensity, as well as with Kuroshio Current strength, make it possible to tentatively connect the start of a migration from Taiwan by sea at the end of the third millennium BCE with the onset of the modern ENSO, which might have weakened the Kuroshio Current offshore eastern Taiwan (Ujiié et al. 2003). Indeed, during an El Niño phase, the bifurcation of the western North Equatorial Current moves to the North (Figure 8), enhancing the strength of the Mindanao Current and weakening that of the Kuroshio Current (Kashino et al. 2005; Kessler and Cravatte 2013; Kim et al. 2004; Hu et al. 2015). For example, research cruises in May/June 2011 and April/May 2012 allowed observing that the Kuroshio transport off the northeast coast of Luzon was roughly 60% greater during La Niña phase than in the more neutral phase of 2011 (Gordon 2012). A weakened Kuroshio Current may thus have greatly benefited the Austronesians of Taiwan, enabling them to migrate first to the Yaeyama Islands and then to the Luzon and Batanes Islands.

At the scale of the entire SCS basin, the dispersion of Taiwan-related Neolithic culture can be highlighted by the dispersion of nephrite (jade) bracelets and tools (Hung et al. 2007). The dispersion of jade from Taiwan could be described as follows : (1), Out-of-Taiwan migration to the Philippines and Borneo starting around 4000 BP, before the peak of jade production in Taiwan (ca. 3500-2500 BP), with continuous interactions between Taiwan and Island Southeast Asia up to Metal age, without producing earring jade artifacts; (2) Export of jade blank starting during the first millenium BC, in connection with Metal Age development in Mainland and Island Southeast Asia around 500 BC, with two main style of earrings distributed all around the SCS region, but faintly found in Taiwan besides Ludao and Lanyu areas. When comparing this dispersion pattern with the seasonality of the coastal surface currents around the South China Sea (Figs. 3 and 8), the Taiwanese nephrite may have been

preferentially spread following an eastern route by sea across the Luzon Strait to the Philippines, and Mindoro, Palawan, and Borneo. The dissemination routes of Taiwan nephrite to Vietnam, Cambodia, and Thailand remains more obscure, with a northern route along the Guangdong current is usually not considered by archeologists because of lack of findings of such artefacts in Hainan, Guangdong, and west coast of Taiwan. The Austronesian's marine activity in the northern part of the SCS, like in north of central Vietnam is still very much of mystery, even though the possibility of round trips can also be envisaged on a seasonal basis with the alternations of summer and winter currents along the borders of the SCS (Fig. 8). Indeed, Yokoyama et al. (2011) showed that this seasonality in the SCS was slightly larger during mid-Holocene than at present, under the monsoon forcing.

5. Conclusions

In this paper, we question whether the present-day environmental conditions in the vicinity of Taiwan and in the South China Sea were already prevailing during mid-Holocene, at the time when human groups migrated from Taiwan to the northeast (Yaeyama Islands), and to the south (Luzon and Batanes islands). Starting from the present-day situation, this paper reviews the geomorphology and the wind patterns and oceanic currents in the South China Sea, focusing on the region around Taiwan. The mid-Holocene conditions were essentially similar to the present ones, and not particularly favorable to sail out of Taiwan either to the Yaeyama Islands or to the Batanes/Luzon region mainly because of the strong Kuroshio Current. We suggest that ENSO variations may have played a significant role in reducing the strength of this major oceanic current during El Niño phases, offering time windows with more favorable sailing conditions to Austronesian populations voyaging from Taiwan.

References

Abram, N.J., McGregor, H.V., Gagan, M.K., Hantoro, W.S., and Suwargadi, B.W., 2009. Oscillations in the southern extent of the Indo-Pacific Warm Pool during the mid-Holocene. Quaternary Science Reviews, 28, 2794-2803.

Allen, M.S., (2006), New ideas about late Holocene climate variability in the central Pacific: Current Anthropology, 47, 521-35.

An, Z., 2000. The history and variability of the East Asian paleomonsoon climate. *Quaternary Science Reviews*, Vol.19, (January 2000), 171-187.

An Z., A., Wu G., Li J., Sun Y., Liu Y., Zhou W., Cai Y., Duan A., Li L., Mao J., Cheng H., Shi Z., Tan L., Yan H., Ao H., Chang H., Feng J., 2015. Global Monsoon Dynamics and Climate Change. Annual Rev. Earth Planet. Sci. 43, 29-77.

Anderson, A., 2005. Crossing the Luzon Strait: archaeological chronology in the Batanes Islands, Philippines and the regional sequence of Neolithic dispersal. Journal of Austronesian Studies, 1(2), 25-44.

Anderson, A., Chappell, J., Gagan, M.K., and Grove, R., 2006. Prehistoric maritime migration in the Pacific islands: an hypothesis of ENSO forcing. Holocene, 16, 1-6.

Behre, K.-E., 2003. Eine neue Meeresspiegelkurve für die südliche Nordsee. Probleme der Küstenforschung im südlichen Nordseegebiet 28.

Bellwood, P., 1997. Prehistory of the Indo-Malaysian Archipelago. Honolulu: University of Hawaii Press.

Bellwood, P. S., 2005. The early movements of Austronesian-speaking peoples in the Indonesian region. Indonesian Institute of Sciences (LIPI).

Bellwood, P., Gamble, C., Le Blanc, S. A., Pluciennik, M., Richards, M., Terrell, J. E., 2007. First Farmers: the Origins of Agricultural Societies, by Peter Bellwood. Malden (MA): Blackwell, 360 pp., 59 figs., 3 tables. Cambridge archaeological journal, 17(01), 87-109.

Bellwood, P., and Dizon, E. (eds.), 2013. 4000 years of migration and cultural exchange: The archaeology of the Batanes Islands, Northern Philippines (Vol. 40). ANU E Press.

Berdin, R. D., Siringan, F. P., Maeda, Y., 2003. Holocene relative sea-level changes and mangrove response in southwest Bohol, Philippines. Journal of Coastal Research 19 304–13.

Blust, R., 1997. Subgrouping, circularity and extinction: Some issues in Austronesia comparatif linguistics. In Zeitoun, E., and Li, P.K.J. (eds): Selected papers from the eighth international conference on Austronesian linguistics. Taipei, Taiwan: Academia Sinica, 1-54.

Brown, J., Collins, M., Tudhope, A.W., Toniazzo, T., 2008. Modelling mid-Holocene tropical climate and ENSO variability: towards constraining predictions of future change with palaeo-data: Climate Dynamics, 30, 19-36.

Carré, M., Sachs, J.P., Purca, S., Shauer, A.J., Braconnot, P., Falcon, R.A., Julien, M., Lavallée, D., 2014. Holocene history of ENSO variance and asymmetry in the eastern tropical Pacific. Science 345, 1045-1048.

Caseldine, C. J., Turney, C., 2010. The bigger picture: towards integrating palaeoclimate and environmental data with a history of societal change. Journal of Quaternary Science, 25, 88–93.

Centurioni, L. R., Niiler, P. P., Lee, D. K., 2004. Observations of inflow of Philippine Sea surface water into the South China Sea through the Luzon Strait. Journal of Physical Oceanography, 34(1), 113-121.

Chang, K.-C., 1989. The Neolithic Taiwan Strait. Kaogu, 6, 541-550.

Chao, S.-Y., P.-T. Shaw, Wu, S. Y., 1996. El Niño modulation of the South China Sea circulation, Prog. Oceanogr., 38, 51–93.

Chen,, Y.G., Liu, T.K., 1996. Sea level changes in the last several thousand years, Penghu Islands, Taiwan Strait. Quaternary Research 45, 254–262.

Chen, Y.G., Liu, T.K., 2000. Holocene uplift and subsidence along an active tectonic margin, southwestern Taiwan. Quaternary Science Reviews 19, 923–930.

Chen, S., Hoffmann, S.S., Lund, D.C., Cobb, K.M., Emile-Geay, J., Adkins, J.F., 2016. A high-resolution speleothem record of western equatorial Pacific rainfall: Implications for Holocene ENSO evolution. Earth and Planetary Science Letters 442, 61-71.

Clement, A. C., R. Seager, Cane, M. A., 1999. Orbital controls on ENSO and the tropical climate. Paleoceanography, 14 (4), 441-456.

Cobb, K. M., Westphal, N., Sayani, H. R., Watson, J. T., Di Lorenzo, E., Cheng, H., ... Charles, C. D., 2013. Highly variable El Niño–Southern Oscillation throughout the Holocene. Science, 339(6115), 67-70.

Conroy, J.L., Overpeck, J.T., Cole, J.E., Shanahan, T.M., Steinitz-Kannan, M., 2008. Holocene changes in eastern tropical Pacific climate inferred from a Galápagos lake sediment record. Quat. Sci. Rev. 27, 1166–1180.

Diamond, J., Bellwood, P., 2003. Farmers and their languages: the first expansions. Science, 300(5619), 597-603.

Deng, Y., Shi, P., Zhou, W., Du, Y., Xie, Q., Zhuang, W., Wang, D., 2012. A dipole wind curl pattern induced by Taiwan Island and its effect on upper stratification in the northeastern South China Sea. Chinese Journal of Oceanology and Limnology, 30, 944-952.

DiNezio, P. N., Tierney, J. E., 2013. The effect of sea level on glacial Indo-Pacific climate, Nature Geoscience 6, 485–491.

Emile-Geay, J., M. A. Cane, R. Seager, Almasi, P., 2007. El Niño as a mediator of the solar influence on climate,Paleoceanography, 22, 3, doi:10.1029/2006PA001304.

Erlandson, J., 2010. Neptune's children: the evolution of human seafaring. In: Anderson, A., Barrett, J. H., Boyle, K. V. (Eds), The global origins and development of seafaring, Cambridge, The MacDonald Institute for Archaeological Research, 19-27.

Fairbanks, R.G., 1989. A 17000-year glacio-eustatic sea level record: influence of glacial melting rates on the Younger Dryas event and deep-ocean circulation. Nature 342, 637–642.

Fang G., Chen, H., Wei, Z., Wang, Y., Wang, X., Li, C., 2006. Trends and interannual variability of the South China Sea surface winds, surface height, and surface temperature in the recent decade. Journal of Geophysical Research, 111 (C11S16).

Fang, W., Guo, J., Shi, P., Mao, Q., 2006. Low frequency variability of South China Sea surface circulation from 11 years of satellite altimeter data. Geophysical research letters, 33(22).

Gordon, A.L., 2012. ENSO sensitive ITF and Kuroshio. American Geophysical Union, Fall Meeting 2012, abstract #OS44B-01.

Goto, K., Kawana, T., Imamura, F., 2010. Historical and geological evidence of boulders deposited by tsunamis, southern Ryukyu Islands, Japan. Earth-Science Reviews, 102(1), 77-99.

Goodwin, I. D., Browning, S. A., Anderson, A. J., 2014. Climate windows for Polynesian voyaging to New Zealand and Easter Island. Proceedings of the National Academy of Sciences, 111(41), 14716-14721.

Hanebuth, T., Stattegger, K., Grootes, P.M., 2000. Rapid flooding of the Sunda Shelf: a late-glacial sea-level record. Science 288, 1033–1035.

Haug, G.H., Hughen, K.A., Sigman, D.M., Peterson, L.C., Rohl, U., 2001. Southward migration of the intertropical convergence zone through the Holocene. Science, v. 293, p. 1304-1308.

Hsieh, M.-L., Liew, P.-W., Hsu, M.-Y., 2004. Holocene tectonic uplift on the Hua-tung coast, eastern Taiwan. Quaternary International, 115-116, 47-70.

Hu, D., Wu, L., Cai, W., Gupta, A. S., Ganachaud, A., Qiu, B., Gordon, A.L., Lin, X., Chen, Z., Hu, S., Wang, G., Wang, Q., Sprintall, J., Qu, T., Kashino, Y., Wang, F., Kessler, W.S., 2015. Pacific western boundary currents and their roles in climate. Nature, 522(7556), 299-308.

Hu, J., Kawamura, H., Hong, H., Qi, Y., 2000. A review on the currents in the South China Sea: seasonal circulation, South China Sea warm current and Kuroshio intrusion. Journal of Oceanography, 56(6), 607-624.

Hu, J., Kawamura, H., Li, C., Hong, H., Jiang, Y., 2010. Review on current and seawater volume transport through the Taiwan Strait. Journal of Oceanography, 66(5), 591-610.

Huang, C.Y., Liew, P.M., Zhao, M., Chang, T.C., Kuo, C.M., Chen, M.T., Wang, C.H. and Zheng, L.F., 1997. Deep sea and lake records of the southeast Asian paleomonsoons for the last 25 thousand years. Earth Planet. Sci. Lett., 146, 59–72.

Hudson, M. J. (2017). The Ryukyu Islands and the Northern Frontier of Prehistoric Austronesian Settlement. terra australis 45, 189-199.

Hung, H. C., Iizuka, Y., Bellwood, P., Nguyen, K. D., Bellina, B., Silapanth, P., Dizon, E., Santiago, R., Datan, I., Manton, J. H., 2007. Ancient jades map 3,000 years of prehistoric exchange in Southeast Asia. Proceedings of the National Academy of Sciences, 104(50), 19745-19750.

Irwin, G., Flay, R.G.J., 2015. Pacific colonisation and canoe performance: Experiments in the science of sailing. Journal of the Polynesian Society, 124(4), 419-443.

Jian, Z., Wang, P., Saito, Y., Wang, J., Pflaumann, U., Oba, T., Cheng, X., 2000. Holocene variability of the Kuroshio Current in the Okinawa Trough, northwestern Pacific Ocean. Earth and Planetary Science Letters 184, 305-319.

Kashino, Y., España, N., Syamsudin, F., Richards, K. J., Jensen, T., Dutrieux, P., Ishida, A., 2009. Observations of the North Equatorial current, Mindanao current, and Kuroshio current system during the 2006/07 El Niño and 2007/08 La Niña. Journal of oceanography, 65(3), 325-333.

Kessler, W.S., 2006. The circulation of the eastern tropical Pacific: A review. Progress in Oceanography, 69, 181-217.

Kessler, W. S., Cravatte, S., 2013. ENSO and short-term variability of the South Equatorial Current entering the Coral Sea. Journal of Physical Oceanography, 43(5), 956-969.

Kim, Y. Y., Qu, T., Jensen, T., Miyama, T., Mitsudera, H., Kang, H. W., Ishida, A., 2004. Seasonal and interannual variations of the North Equatorial Current bifurcation in a high-resolution OGCM. Journal of Geophysical Research: Oceans, 109(C3).

Koutavas, A., deMenocal, P.B., Olive, G.C., Lynch-Stieglitz, J., 2006. Mid-Holocene El Nin˜o–Southern Oscillation (ENSO) attenuation revealed by individual foraminifera in eastern tropical Pacific sediments. Geology 12, 993-996.

Kutzbach JE, Guetter P. J., 1986. The influence of changing orbital parameters and surface boundary conditions on climate simulations for the past 18 000 years. J. Atmos. Sci., 43, 1726–1759.

Lape, P. V., O'Connor, S., Burningham, N., 2007. Rock Art: A potential source of information about past maritime technology in the south-east Asia Pacific region. International Journal of Nautical Archeology, 36, 238-253.

Leduc G., Vidal L., Cartapanis O., Bard E., 2009. Modes of Eastern Equatorial Pacific thermocline variability: Implications for ENSO dynamics over the last glacial period. Paleoceanography, 24, PA3202, doi:10.1029/2008PA1701.

Leduc, G., Schneider, R.R., Kim, J.-H., Lohmann, G., 2010. Holocene and Eemian sea surface temperature trends as revealed by alkenone and Mg/Ca paleothermometry. Quaternary Science Reviews, 29, 989-1004.

Liang, W. D., Jan, J. C., Tang, T. Y., 2000. Climatological wind and upper ocean heat content in the South China Sea. Acts Oceanogr. Taiwan, 38, 91-114.

Liew, P.M., Huang, S.Y. and Kuo, C.M., 2006a. Pollen stratigraphy, vegetation and environment of the Last Glacial and Holocene - A record from Toushe Basin, central Taiwan. Quat. Int., 147, 16–33.

Liew, P.M., Huang, S.Y. and Kuo, C.M., 2006b. Holocene thermal optimal and climate variability of East Asian monsoon inferred from forest reconstruction of a subalpine pollen sequence, Taiwan. Earth Planet. Sci. Lett., 250, 596–605.

Liew, P.M., Kuo, C.M., Huang, S.Y. and Tseng, M.H., 1998. Vegetation change and terrestrial carbon storage in eastern Asia during the Last Glacial Maximum as indicated by a new pollen record from central Taiwan. Glob. Planet. Change, 16–17, 85–94.

Liu W T, Xie X. 1999. Space-based observations of the seasonal changes of South Asian monsoons and oceanic response. Geophys. Res. Lett., 26: 1 473-1 476.

Liu K.-K., Chao S.-Y., Shaw P.-T., Gong G.-C., Chen C.-C. and Tang T.Y. 2002. Monsoon-forced chlorophyll distribution and primary production in the South China Sea: observations and a numerical study. Deep-Sea Res. I 49: 1387–1412.

Madhi, W., 2013. Pre-Austronesian origins of seafaring in insular southeast Asia. In: Acri, A., Landmann, A. (Eds), Cultural transfers in historical maritime Asia: Austronesian-Indic Encounters, ISEAS Publishing, Singapore, 1-30.

Maeda, Y., Siringan, F., Omura, A., Berdin, R., Hosono, Y., Atsumi, S., Nakamura, T., 2004. Higher-than-present Holocene mean sea levels in Ilocos, Palawan and Samar, Philippines. Quaternary International 115 15–26.

Marchitto, T.M., Muscheler, R., Ortiz, J.D., Carriquiry, J.D., van Geen, A., 2010. Dynamical response of the tropical Pacific Ocean to solar forcing during the Holocene. Science 330, 1378–1381.

Masson-Delmotte V., Schulz M., Abe-Ouchi A., Beer J., Ganopolski A., González Rouco J.F., Jansen E., Lambeck K., Luterbacher J., Naish T., Osborn T., Otto-Bliesner B., Quinn T., Ramesh R., Rojas M., Shao X., Timmermann A., 2013. Information from Paleoclimate Archives. in: Stocker T.F., Qin D. , Plattner G.-K., Tignor M., Allen S.K., Boschung J., Nauels A., Xia Y., Bex V., Midgley P.M., eds. Climate Change 2013: The Physical Science Basis. Contribution of Working Group I to the Fifth Assessment Report of the Intergovernmental Panel on Climate Change. Cambridge University Press, Cambridge, UK, New York, NY, USA.

McGregor, H.V., Fischer, M.J., Gagan, M.K., Fink, D., Phipps, S.J., Wong, H., Woodroffe, C.D., 2013. A weak El Niño/Southern Oscillation with delayed seasonal growth around 4300 years ago. Nat. Geosci. 6 (11), 949.

McPhaden, M.J., 2015. Playing hide and seek with El Niño. Nature Climate Change, 5, 791-795.

Meyer A., K. Rege, 2011. Blue Marble 3000. Visualization developed at the Zurich University of Applied Sciences (http://radar.zhaw.ch/bluemarble3000_en.html), as of 7th of March 2016.

Mohtadi M., Oppo D.W., Steinke S., Stuut J-B W., De Pol-Holz R., Hebbeln D., Lückge A., 2011. Glacial to Holocene swings of the Australian-Indonesian monsoon. Nature Geoscience 4, 540-544.

Moy, C.M., Seltzer, G.O., Rodbell, D.T., Anderson, D.M., 2002. Variability of El Niño/Southern Oscillation activity at millennial timescales during the Holocene epoch. Nature 420, 162-165.

Montenegro, A., Callaghan, R.T., Fitzpatrick, S.M., 2016. Using seafaring simulations and shortest-hop trajectories to model the prehistoric colonization of Remote Oceania.

Murray-Wallace, C.V., Woodroffe, C.D., 2014. Quaternary sea-level changes: a global perspective. Cambridge University Press, 504 pages.

Nakamura, M., 2006. Source fault model of the 1771 Yaeyama tsunami, southern Ryukyu Islands, Japan, inferred from numerical simulation. pure and applied geophysics, 163(1), 41-54.

Nunn, P. D., Carson, M. T., 2015. Sea-level fall implicated in profound societal change about 2570 cal yr BP (620 BC) in Western Pacific Island groups. Geography and Environment, doi: 10.1002/geo2.3.

O'Connor, S., 2007. New evidence from East Timor contributes to our understanding of earliest modern human colonization east of the Sunda Shelf. Antiquity, 81, 523-535.

O'Connell, J. F., Allen, J., Hawkes, K., 2010. Pleistocene Sahul and the origins of seafaring. In: Anderson, A., Barrett, J. H., Boyle, K. V. (Eds), The global origins and development of seafaring, Cambridge, The MacDonald Institute for Archaeological Research, 57-68.

Partin, J.W., Cobb, K.M., Adkins, J.F., Clark, B., Fernandez, D.P., 2007. Millennial-scale trends in west Pacific warm pool hydrology since the Last Glacial Maximum. Nature 449, 452-455.

Pawley, A., and Pawley, M., 1994. Early Austronesian terms for canoes parts and seafaring. In Pawley, A., and Ross, M.D. (eds): Austronesian terminologies: Continuity and change (Pacific Linguistic Series C No. 127). Canberra: Department of Linguistics, Research School of Pacific and Asian Studies, The Australian National University, 329-391.

Phipps, S.J., and Brown, J.N., 2010. Understanding ENSO dynamics through the exploration of past climates: IOP Conference Series: Earth and Environmental Science, 9.

Qiu, Y., Li, L., Chen, C. T. A., Guo, X., Jing, C., 2011. Currents in the Taiwan Strait as observed by surface drifters. Journal of oceanography, 67(4), 395-404.

Rasmusson, E.M., Carpenter, T .H., 1982. Variations in tropical sea surface temperature and surface wind fields associated with the Southern Oscillation / El Niño. Monthly Weather Review 110, 354-384.

Shaw, P. T., Chao, S. Y., 1994. Surface circulation in the South China Sea. Deep Sea Research Part I: Oceanographic Research Papers, 41(11), 1663-1683.

Siame, L.L., Chu, H.-T., Carcaillet, J., Lu, W.-C., Bourlès, D.L., Braucher, R., Angelier, J., Dussouillez, P, 2007. Glacial retreat history of Nanhuta Shan (North-east Taiwan) from preserved glacial features: the Cosmic ray exposure perspective. Quaternary Science Reviews, 26, 2185-2200.

Simanjuntak, T. (2017). The Western Route Migration: A Second Probable Neolithic Diffusion to Indonesia. Terra Australis, 45, 201-212.

Summerhayes, G. R., Anderson, A., 2009. An Austronesian presence in southern Japan: early occupation in the Yaeyama islands. Bulletin of the Indo-Pacific Prehistory Association, 29, 76-91.

Tjallingii, R., Stattegger, K., Wetzel, A., Van Phach, P., 2010. Infilling and flooding of the Mekong River incised valley during deglacial sea-level rise. Quaternary Science Reviews, 29, 1432-1444.

Tudhope, A. W., Chilcott, C. P., McCulloch, M. T., Cook, E. R., Chappell, J., Ellam, R. M., ... Shimmield, G. B., 2001. Variability in the El Niño-Southern Oscillation through a glacial-interglacial cycle. Science, 291(5508), 1511-1517.

Ujiié, Y., Ujiié, H., Taira, A ., Nakamura, T., Oguri, K., 2003. Spatial and temporal variability of surface water in the Kuroshio source region, PacificOcean, over the past 21,000 years : evidence from planktonic foraminifera. Marine Micropaleontology 49, 335-364.

Wang, P., Li, Q., 2009. Oceanographical and geological background. *In:* Wang, P., and Li Q. (Eds), the South China Sea, Developments in Paleoenvironmental Research 13, Spinger Science, 25-68.

Wang G., Chen D. and Su J. 2006. Generation and life cycle of the dipole in the South China Sea summer circulation. J. Geophys. Res. 111: C06002.

Wang G, Chen D, Su J. 2008. Winter eddy genesis in the eastern South China Sea due to orographic wind jets. J. Phys. Oceanogr., 38: 726-732.

Wang, B., Wu, R., Fu, X., 2000. Pacific-East Asian teleconnection: How does the ENSO affects East Asian climate? J. Clim., 13, 1517-1536.

Wang, P., Clemens, S., Beaufort, L., Braconnât, P., Ganssen, G., Jian, Z., Kershaw, P., Sarnthein, M., 2005. Evolution and variability of the Asian monsoon system: state of the art and outstanding issues. Quaternary Science Reviews, 24, 595-629.

Wang, Y.J., Cheng, H., Edwards, R.L., He, Y.Q., Kong, X.G., An, Z.S., Wu, J.Y., Kelly, M.J., Dykoski, C.A., Li, X.D., 2005. The Holocene Asian monsoon: links to solar changes and North Atlantic climate. Science 308, 854–857.

Webster, P.J., Magaña, V.O., Palmer, T.N., Shukla, J., Tomas, R.A., Yanai, M., Yasunari, T., 1998. Monsoons : Processes, predictability, and the prospects for predicion. Journal of Geophysical Research, 103, 14451-14510.

Wells, P. E., Wells, G. M., 1994. Large-scale reorganization of ocean currents offshore Western Australia during the late Quaternary. Marine Micropaleontology, 24(2), 157-186.

Wei, K.Y., 2002. Environmental changes during the late Quaternary in Taiwan and adjacent seas: An overview of recent results of the past decade (1990-2000). Western Pacific Earth Sci., 2, 149–160.

Wilmshurst, J. M., Hunt, T. L., Lipo, C. P., Anderson, A. J., 2011. High-precision radiocarbon dating shows recent and rapid initial human colonization of East Polynesia, PNAS. 108 (5), 1815-1820.

Wu, B., J. Wang, J., 2002. Winter Arctic Oscillation, Siberian High and East Asian Winter Monsoon. Geophys. Res. Lett., 29(19), 1897, doi:10.1029/2002GL015373.

Wyrwoll, K.H., Miller, G.H., 2001. Initiation of the Australian summer monsoon 14,000 years ago. Quaternary International, 83(5), 119-128.

Xue, H., Chai, F., Pettigrew, N., Xu, D., Shi, M., Xu, J., 2004. Kuroshio intrusion and the circulation in the South China Sea. Journal of Geophysical Research 109(C2017).

Yancheva, G., Nowaczyk, N. R., Mingram, J., Dulski, P., Schettler, G., Negendank, J. F.W., Liu, J., Sigman, D. M., Peterson, L. C., Haug, G. H., 2007. Influence of the intertropical convergence zone on the East Asian monsoon. Nature, 445, 74–77.

Yi, S., 2011. Holocene vegetation responses to East Asian monsoonal changes in South Korea. In: Blanco, J., Kheradmand, H. (Eds), Climate Change - Geophysical Foundations and Ecological Effects, Publisher: InTech, 534 pages, doi: 0.5772/23920.

Yokoyama, Y., Suzuki, A., Siringan, F., Maeda, Y., Abe-Ouchi, A., Ohgaito, R., Kawahata, H., Matsuzaki, H., 2011. Mid-Holocen palaeoceanography of the northern South China Sea using coupled fossil-modern coral and atmosphere-ocean GCM model. Geophysical Research Letters, 38, L00F03, doi: 10.1029/2010GL044231.

Zhang, Y., 1997. East Asian winter monsoons: results from eight AMIP models. Clim. Dyn., 13: 11 797-11 820.

Zhang, Z., Leduc, G., Sachs, J. P., 2014. El Niño evolution during the Holocene revealed by a biomarker rain gauge in the Galápagos Islands. Earth and Planetary Science Letters, 404, 420-434.